Progress in Reaction Kinetics and Mechanism

ARTICLE

Open Access

https://doi.org/10.48130/prkm-0026-0008

Progress in Reaction Kinetics and Mechanism **2026**, 51: e016

Exploring pyrolysis kinetics of octamethylcyclotetrasiloxane by experiments and ReaxFF molecular dynamics simulations

Neng Wang[1], Junhao Sun[2], Yaosong Huang[2*] and Guoqing Shen[1*]

[1] *School of of Energy Power and Mechanical Engineering, North China Electric Power University, Beijing 102206, China*

[2] *College of Energy, Soochow University, Suzhou 215006, China*

* Correspondence: yshuang@suda.edu.cn (Huang Y); shenguoqing@ncepu.edu.cn (Shen G)

Abstract

The pyrolysis kinetics of octamethylcyclotetrasiloxane (D4) at high temperatures, crucial for silicon-based material synthesis and waste-to-energy applications are not fully understood. This work carries out this research by combining flow tube experiments (803–843 K), with ReaxFF molecular dynamics (MD) simulations (1,500–2,600 K). Experimentally, a significant increase in methane (CH_4) production at 843 K—compared to its absence at 803 K—suggests a high activation energy barrier for CH_4 formation, which is overcome via Si-C bond cleavage, and methyl radical ($\cdot CH_3$) chain reactions. ReaxFF MD simulations indicate that D4 decomposition follows first-order kinetics at high temperatures, with an apparent activation energy of 81.3 ± 4.2 kJ/mol, much lower than the 273.2–320 kJ/mol reported at lower temperatures. This difference arises from the enhancement of the D4 decomposition channel in which radicals participate in at high temperatures. Both experiments and simulations confirm that hydrogen abstraction by $\cdot CH_3$ radicals ($\cdot CH_3 + R\text{-}H \rightarrow CH_4 + R\cdot$) is the primary route for CH_4 production. The developed multi-scale kinetic model offers crucial insights for optimizing silicon-based material synthesis and simulating silicon-containing gas combustion.

Citation: Wang N, Sun J, Huang Y, Shen G. 2026. Exploring pyrolysis kinetics of octamethylcyclotetrasiloxane by experiments and ReaxFF molecular dynamics simulations. *Progress in Reaction Kinetics and Mechanism* 51: e016 https://doi.org/10.48130/prkm-0026-0008

Introduction

Organic silicon compounds, known for their chemical stability and thermodynamic properties are integral to nanomaterial synthesis, chemical vapor deposition (CVD), and flame retardants[1–6]. Among these, octamethylcyclotetrasiloxane (D4, $[CH_3]_8Si_4O_4$]), with the structure unit (-$[CH_3]_2$SiO-), is prevalent. As a key precursor, D4 forms silica nanoparticles or films via high-temperature pyrolysis and oxidation. Its pyrolysis kinetics are crucial for material synthesis efficiency and product characteristics[7]. Additionally, D4 is frequently found in landfill syngas[8–10], yet its use in combustion systems is hindered by the uncertain pyrolysis behavior of silicon compounds, especially D4. The pyrolysis of D4 is intricate, involving numerous intermediates and pathways, leading to an incomplete understanding of its kinetics. Thus, investigating the high-temperature pyrolysis kinetics of D4 is essential for optimizing industrial processes and informing combustion models of complex silicon-based systems.

Recent studies on the pyrolysis kinetics of D4 reveal significant limitations, particularly in temperature and pressure ranges. Davidson & Thompson[11] investigated D4 decomposition in a static reactor at low temperatures (762–842 K), proposing a mechanism for D3 formation via dimethyl siloxane monomer (D1) elimination, with an activation energy of 301 kJ/mol. However, this research did not address kinetic behavior at higher temperatures (> 1300 K), crucial for nanomaterial synthesis[12]. Sanogo & Zachariah[7] extended the temperature range (1,058–1,197 K) using a fast flow reactor, identifying a secondary pathway for D5 decomposition into D3 and D2, yet the mechanism did not fully elucidate methane (CH_4) formation. Additionally, intermediate detection remains challenging, with ongoing debate over the reaction pathway. Khabashesku et al.[13] identified D3, SiO, and small hydrocarbons in D4 pyrolysis products via matrix-isolated infrared spectroscopy, but failed to directly observe the key intermediate D1, suggesting its rapid decomposition into SiO and free radicals. Almond et al.[14], using G3-level quantum chemical calculations, suggested that D1 decomposes into CH_3 and CH_3SiO via Si-C bond cleavage, initiating a chain reaction that produces CH_4 and C_2H_2. However, the stability and decomposition pathway of D1 at high temperatures remained disputed, particularly the direct formation of CH_4, which lacks full validation. Additionally, the mechanism model has its limitations. Sela et al.[12] developed a D4/D3 sub-mechanism comprising 19 reactions between 1,160 and 1,600 K, integrating shock tube experiments with high repetition rate time-of-flight mass spectrometry (HRR-TOF-MS). They observed a significantly higher decomposition rate for D4 compared to D3. Nonetheless, the model underestimates CH_4 experimental values, indicating potentially overlooked rapid channels. Furthermore, discrepancies in predictions for products like C_2H_2, where experimental values exceed simulations, highlight the need for refinement in the secondary reaction pathway.

This study investigates the high-temperature pyrolysis kinetics of D4 using molecular dynamics simulations and gas chromatography, extending its reaction kinetics beyond 1,500 K. It proposes new reaction channels to elucidate the CH_4 generation pathway, enhancing the understanding of CH_4 formation observed by experiments and simulations. By integrating experimental and theoretical approaches, the study unveils the formation and transformation pathways of intermediates, such as the open chain structure I-$Si_4O_4C_8H_{24}$, and clarifies the contribution of some important reactions to pyrolysis kinetics and product distribution. This research aims to elucidate the multi-scale kinetic behavior of D4 during high-temperature pyrolysis, providing a more precise theoretical foundation for the synthesis and combustion simulation of silicon-based materials.

© The Author(s)

Experimental and simulation methods

Experimental setup and product detection

Figure 1 shows the schematic diagram of the experimental setup and product detection of D4 pyrolysis. The experiments were conducted in a flow tube reactor (about 980 cm^3). Argon (Ar) served as the carrier gas to introduce D4 into the reactor. Before each pyrolysis experiment, the reactor was purged with Ar to remove air, with the flow rate of 200 mL/min during heating to the desired temperature. Once enough D4 was introduced, the reactor's front and rear valves were closed to allow complete pyrolysis of D4. After pyrolysis, the valves were reopened, Ar was reintroduced, and pyrolysis products were collected at the quartz nozzle. Throughout this process, the reactor maintained a constant temperature, while liquid D4 was heated to its boiling point in an oil bath and transported into the reactor by Ar. Experiments were conducted at 803 K and 843 K, with products collected and analyzed using gas chromatography. The other conditions included reactor pressure (3–6 MPa), carrier gas flow rate (200 mL/min), D4 vapor feed rate (76 g/min), residence time (60 s), and D4 initial concentration (2.65×10^{-4} mol/mL). In addition, reproducibility tests showed that the uncertainties of measured temperature, pressure, and flow rate were ± 1 °C, ± 0.3 MPa, and ± 2.5 mL/min, respectively.

In the gas chromatograph, pyrolysis products were introduced into the thermal conductivity detector and propelled through the column by a carrier gas, typically hydrogen or helium. Within the chromatographic column, sample components interacted with a stationary phase, such as a silica gel, undergoing adsorption, desorption, and dissolution. Variations in boiling point, polarity, and adsorption properties resulted in different movement speeds, facilitating separation. The separated components entered the detector, which recorded their retention time and peak area. A data processing system then analyzed these metrics to determine component content. Retention time, the duration for a component to reach peak height, correlates with boiling point; higher boiling points result in slower peak times and longer retention. This experiment employed a hydrogen flame ionization detector (FID), with hydrogen supplied by a generator. An external standard method was used for integration, employing the standard gas to create a reference sample.

ReaxFF molecular dynamics simulations

Traditional empirical force fields necessitate predefined atomic connectivity for molecular dynamics simulations and cannot model bond formation or breaking in chemical reactions. In contrast, the ReaxFF force field utilizes 'bond order' based on interatomic distances to simulate complex reactions without preset pathways[15]. This bond order allows ReaxFF to determine interaction parameters, including atomic parameters, bond stretching, angle bending, dihedral twisting, conjugation, coordination corrections, and hydrogen bonding. The electronegativity equalization method (EEM) dynamically updates system charges, enhancing data accuracy. Compared to other key-level methods, ReaxFF offers superior accuracy and reactivity. In ReaxFF, molecular energy is expressed via bond order unless a bond interaction occurs, i.e.,

$$E_{system} = E_{bond} + E_{over} + E_{under} + E_{lp} + E_{val} + E_{tor} + E_{conj} + E_{Coulomb} + E_{vdWaal.} \quad (1)$$

where, E_{system} refers to the total energy of the system, and E_{bond} represents the bond energy. E_{over} and E_{under} represent the energy correction terms for over and under coordination, respectively. E_{lp} represents the energy term for lone pair electrons, and E_{val} represents the energy term for bond angles. E_{tor} represents the energy term for dihedral angles, $E_{vdWaals}$ represents the energy term for van der Waals forces, and $E_{Coulomb}$ represents the energy term for Coulomb forces. The specific expressions for the above energy terms are found in the references[16].

ReaxFF molecular dynamics simulations were performed using the Amsterdam Modeling Suite (AMS) software with a reactive force field from PDMS decomposition[17], previously validated in other organosilicon systems[18,19]. The molecular structure of D4, sourced from the NIST Chemistry WebBook, is depicted in Fig. 2. The size of simulation box was 68 Å × 68 Å × 68 Å, containing fifty D4 molecules at a gas density of 0.07866 g/mL. The simulations employed Canonical Ensemble (NVT) with temperatures ranging from 1,500 to 2,600 K to explore the high-temperature pyrolysis mechanism of D4. Under the NVT ensemble, with a fixed density, the pressure increases with temperature, and the highest pressure can reach about 80 bar. The total simulation duration spanned 100 to 250 ps, with a time step of 0.1 fs, and a bond order cutoff of 0.3 was applied. To improve statistical reliability, it was noted that we had performed three independent runs at each temperature with different initial configurations, and averaged the results to minimize stochastic fluctuations.

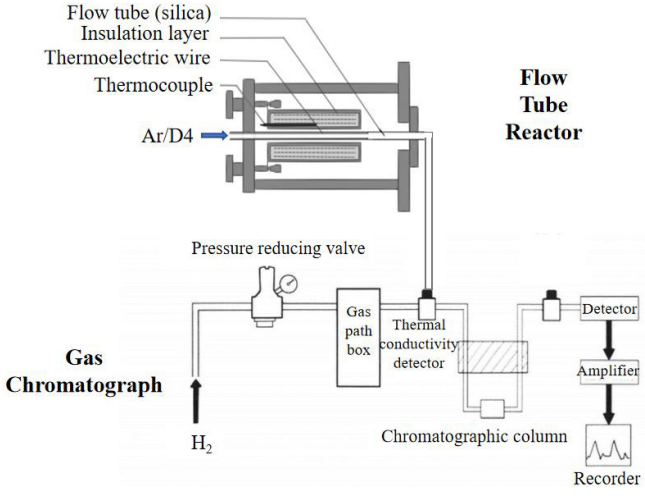

Fig. 1 Experimental setup and product detection of D4 pyrolysis.

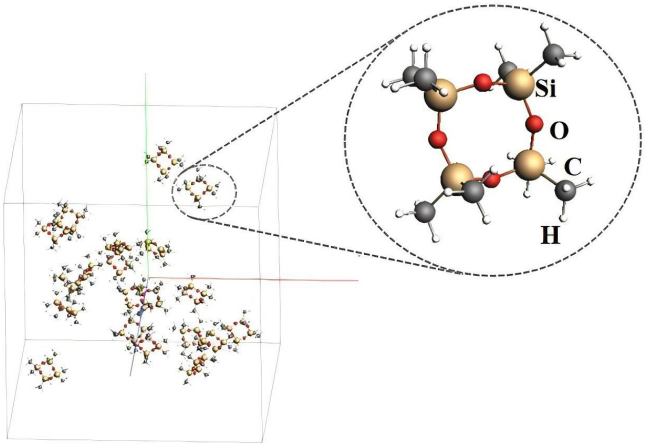

Fig. 2 The initial geometric configuration of D4 pyrolysis for ReaxFF MD simulations.

Additionally, we mainly focused on early-stage kinetics (≤ 200 ps), where D4 decomposition and primary product formation dominate.

Validation of the reactive force field

To verify the accuracy of the force field used in ReaxFF MD simulations, density functional theory (DFT) calculations were conducted with Gaussian 09 software, and the results from DFT calculations were compared with ReaxFF simulations. The B3LYP method with a 6-31G(d) basis set was employed in the DFT calculations. Figure 3 shows the potential energy surface scans at different molecular structures (different bond lengths and angles). Good agreement is obtained between ReaxFF simulations and DFT calculations in the relative energies of different Si-C bond lengths and Si-O bond lengths, and the relatively small errors are presented in most scanning points of Si-O-Si angles and Si-O-Si-O dihedral angles, which indicates that the reactive force field used in the ReaxFF simulations is acceptable.

Results and discussion

Pyrolysis product analysis using gas chromatography

In this section, D4 pyrolysis experiments were conducted at 803 K and 843 K in a flow tube reactor. The hydrocarbon products were analyzed in detail by gas chromatography (GC). Each experiment was repeated three times with identical conditions, and the reproducibility tests indicated that the uncertainties of the measured mole fractions of D4 pyrolysis products was less than ± 0.01%.

Figure 4 shows the chromatographic spectral lines of hydrocarbons produced after D4 pyrolysis at 803 K and 843 K, where the corresponding product names are presented in Table 1. The detailed chromatographic data are shown in Tables 2 and 3. The data clearly reveals that pyrolysis temperature plays a significant role in regulating product distribution, especially the key effect on methane (CH_4) formation. At 803 K, the main products detected are C2-C4 hydrocarbons such as ethane (C_2H_6), ethylene (C_2H_4), propane (C_3H_8), propylene (C_3H_6), butane (C_4H_{10}), and butene (C_4H_8). These products indicate that at this temperature, the initial cleavage of D4 molecules mainly involves the cleavage of Si-O-Si bonds and the migration, recombination, or elimination of methyl (-CH_3) groups, forming free radicals or fragments containing 1 to 2 carbon atoms, which in turn generate the observed C2-C4 alkanes and olefins by recombination, disproportionation, or hydrogen extraction reactions. When the temperature was raised to 843 K, the spectrum of products changed significantly. In addition to the C2-C4 products described above, methane (CH_4) becomes an extremely prominent product (its prominent peak is clearly visible in Fig. 4). This contrast strongly suggests that methane formation is a process with high activation energy in the pyrolysis of D4, and is extremely temperature-sensitive. The temperature of 803 K may be below the effective initiation temperature for this critical path, or its reaction rate may be too low to produce detectable amounts of methane at this temperature. A temperature difference of only 40 K from 803 K (no detection), to 843 K (mass production), results in a significant change in methane from nothing, strongly suggesting the existence of a specific temperature window or activation energy barrier. Below this threshold (e.g., 803 K), the reaction path leading to C2-C4

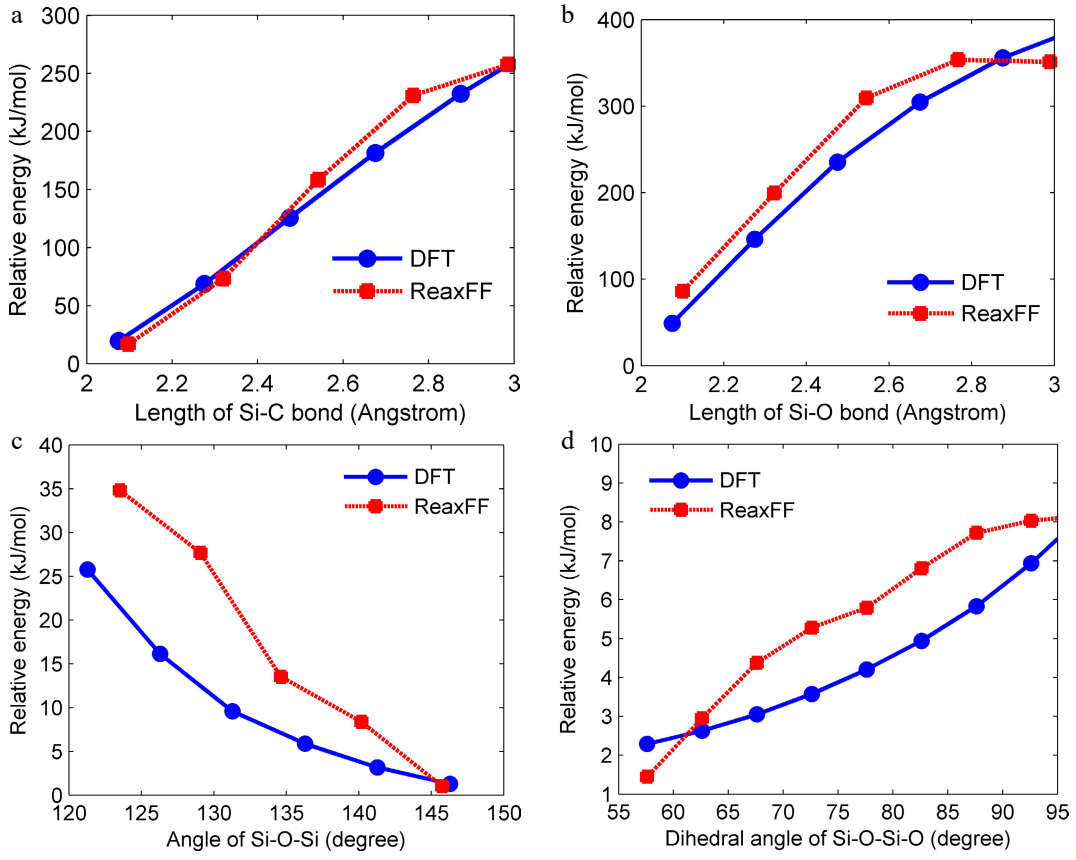

Fig. 3 Potential energy surface scans by ReaxFF simulations and DFT calculations with different bond lengths of (a) Si-C bonds, (b) Si-O bonds, and angles of (c) Si-O-Si bonds, and (d) Si-O-Si-O bonds. The relative energy is obtained by subtracting the initial molecular structure energy.

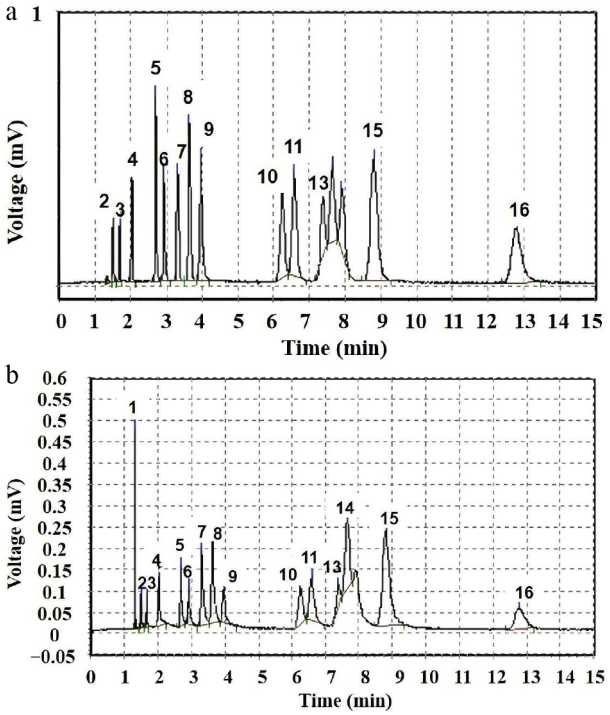

Fig. 4 The detected results of hydrocarbons from D4 pyrolysis by gas chromatography, where (a) and (b) correspond to the temperatures of 803, and 843 K, respectively.

Table 1. Component names represented by peak number in gas chromatograms.

Peak No.	Component name	Peak No.	Component name
1	Methane	9	Propadiene
2	Ethane	10	1-Butene
3	Ethylene	11	trans-2-Butene
4	Propane	12	Isobutylene
5	Cyclopropane	13	iso-Pentane
6	Propylene	14	cis-2-Butene
7	Isobutane	15	n-Pentane
8	n-Butane	16	1,3-Butadiene

Table 2. Chromatographic data of pyrolysis products at 803 K.

Peak no.	Retention time (min)	Peak height (μV)	Peak area (μV·s)	Mole fraction (%)
1	/	/	/	/
2	1.515	237.000	414.300	0.0131
3	1.682	195.500	380.200	0.0134
4	2.032	398.458	922.800	0.0215
5	2.698	703.759	2,155.450	0.0434
6	2.932	408.000	1,415.500	0.0337
7	3.315	400.000	1,644.500	0.0369
8	3.640	579.756	2,698.850	0.0447
9	3.965	450.385	2,339.200	0.0531
10	6.240	308.933	2,575.000	0.0497
11	6.582	373.814	3,285.500	0.0599
12	7.382	213.667	1,584.700	0.0395
13	7.640	278.303	2,327.700	0.0449
14	7.907	227.150	2,038.000	0.0393
15	8.807	450.358	6,256.600	0.0678
16	12.798	193.846	3,925.900	0.0646

Note: Argon is the primary species in the gas mixture.

Table 3. Chromatographic data of pyrolysis products at 843 K.

Peak no.	Retention time (min)	Peak height (μV)	Peak area (μV·s)	Mole fraction (%)
1	1.323	453.000	738.900	0.0763
2	1.507	78.167	170.900	0.0054
3	1.673	77.600	167.750	0.0059
4	2.023	111.909	388.800	0.0090
5	2.690	144.276	532.450	0.0107
6	2.923	90.135	389.500	0.0093
7	3.315	177.308	980.700	0.0161
8	3.640	200.472	1,165.600	0.0193
9	3.965	75.037	467.900	0.0106
10	6.257	85.795	780.750	0.0151
11	6.598	100.742	1,009.600	0.0184
13	7.390	50.371	365.200	0.0091
14	7.657	157.459	1,475.000	0.0502
15	8.798	220.842	3,427.950	0.0372
16	12.790	48.941	978.600	0.0161

products dominate; above this threshold (e.g., 843 K), new pathways leading to methane formation are opened or accelerated.

The possible methane formation pathways include: (1) direct dehydrogenation/cleavage of methyl radicals. Higher temperatures lead to higher energy collisions, which may prompt the methyl radical ($\cdot CH_3$) produced by the cleavage of D4 to directly abstract hydrogen atoms from other molecules (e.g., another methyl group, a silomethyl group, or a larger hydrocarbon radical) to form CH_4. For example: $\cdot CH_3$ + R-H -> CH_4 + R· (R-H may be another methylsilyl group, intermediate molecule, or product molecule); (2) deep cleavage of the silyl group. D4 cleavage initially produces Si-CH_3 bonds containing intermediates (e.g. silicon radical $R_3Si\cdot$ or silylene R_2Si:). At elevated temperatures, the Si-CH_3 bond on these intermediates may undergo homolysis to produce methyl radicals ($\cdot CH_3$), which can then rapidly participate in the reaction to form CH_4 (e.g., hydrogen extraction reaction above, or a combination with other methyl radicals to form ethane; but ethane is already present at 803 K, indicating that methyl radical formation has occurred at 803 K, but not enough, or different routes make CH_4 difficult to form). The more critical high temperature pathway may be the direct cleavage of Si-C bonds accompanied by H transfer: Si-CH_3 → Si· + $\cdot CH_3$ (this step may be slower at lower temperatures), or more complex intramolecular rearrangement leading to direct removal of CH_4, and high temperature provides sufficient energy for Si-C bond cleavage; (3) secondary reactions are enhanced. The initial C2-C4 olefins (such as ethylene and propylene) are less stable at high temperatures, and further cracking, dehydrogenation, or radical attack reactions may occur. These secondary reactions may also contribute to CH_4. For example, pyrolysis or radical-induced cracking of ethylene can produce methyl radicals and methylene groups, which in turn produce methane. Higher free radical concentrations at 843 K may also promote such secondary reactions.

From 803 K (dominated by C2-C4), to 843 K (dominated by C2-C4 + CH_4), the transition of product distribution modes, and the reconstruction of D4 pyrolysis paths with temperature are clearly demonstrated. The presence of methane marks a significant increase in the depth of pyrolysis, involving higher energy demand bond breakage (e.g., Si-C bond homolysis, methyl deep dehydrogenation) or more intense secondary reactions. In addition, the extreme sensitivity of methane formation to temperature indicates that the reaction path has a high apparent activation energy. This experimental phenomenon provides a key constraint condition for the subsequent construction of a detailed D4 pyrolysis model, which must include elementary reaction steps that become important only at

high temperatures, and accurately describe CH_4 formation (e.g., specific Si-C bond cleavage, rapid hydrogen extraction of methyl radicals, etc.). The main microscopic mechanism leading to CH_4 formation and silicon-containing species detection can be observed by ReaxFF MD simulations.

A single molecule pyrolysis by ReaxFF MD simulations

To understand the chemical bond breaking of the D4 molecule, a single-molecule pyrolysis was investigated using the ReaxFF molecular dynamics simulation method, and the pyrolysis pathway was analyzed. The total simulation duration was 200 ps using the NVT ensemble, and the time step was 0.2 fs. A pyrolysis temperature of 2,000 K was employed for accelerating the occurrence of chemical reactions.

The pyrolysis pathway of a single D4 molecule is shown in Fig. 5. The initial step of pyrolysis is the cleavage of the Si–C bond to remove the methyl group, as in reaction R1. This is because the bond energy of the Si-C bond (about 377 kJ/mol) is weaker than that of other chemical bonds (such as the Si-O bond at 540 kJ/mol)[7], so this bond breaks first when pyrolysis occurs. Subsequently, a ring-opening reaction of the molecule takes place, that is, the Si-O bond breaks, causing the molecule to transform into a ring- opening structure, as in reaction R2. Thereafter, another methyl group is removed and one of the methyl groups is transferred; the removed methyl group is located on the Si atom, attached to the O atom on the O side of the just broken Si-O bond, as shown in reaction R3. The transferred methyl group is located on one of the Si atoms of the unbroken Si-O bond, and is transferred to the Si atom of the just broken Si-O bond, as shown in reaction R4. Further, the molecule undergoes a dehydrogenation reaction to lose a hydrogen atom (R5), in which the C-H bond is broken because the bond energy of the C-H bond is greater, relative to the Si-C bond and the Si-O bond. The methyl group (methylene CH_2) that loses a hydrogen atom is also removed, as in reaction R6. A series of demethylation reactions (R7 to R10) then occur, leaving only one methyl group on the final molecule. $CH_3O_4Si_4$ molecules are then formed through ring-opening and H-transfer reactions. The $CH_3O_4Si_4$ molecule then decomposes into HO_4Si_3 and CH_2Si. Through ReaxFF molecular dynamics simulation, it is found that these two substances are the final products of single-molecule pyrolysis of D4 at 2,000K and cannot be decomposed again. It can be seen from the energy evolution of Fig. 6 that when pyrolysis proceeds to reaction R13, the overall energy of molecules maintains relative equilibrium. To decompose these two products further, it is necessary to increase the pyrolysis temperature. The study of a single molecule pyrolysis can not only clarify the reactions caused by chemical bond breakage, but also help to explain the pyrolysis reaction path of actual D4 precursor.

Pyrolysis kinetics of D4 by ReaxFF MD simulations

In this section, the pyrolysis kinetics of D4 was investigated under the condition of 50 molecules, and gas density of 0.07866 g/ml using the ReaxFF molecular dynamics simulations at a temperature range of 1,500–2,600 K. The simulation time is set to 150–250 ps and the time step is 0.1 fs.

Figure 7 shows the variation of D4 molecular number with time at different temperatures. Results showed that the decomposition rate of D4 increased significantly with the increase in temperature. At 1,500 K, only about 25% of D4 decomposes within 250 ps, while at 2,600 K, the decomposition is basically completed within 150 ps, which accords with the basic law of high temperature promoting reactions. By fitting the D4 concentration decay curve, it was found that the D4 pyrolysis followed a first-order reaction kinetics model[3], i.e.,

$$\frac{dn}{dt} = -k_{dec}n \quad (2)$$

where, k_{dec} is the rate constant for D4 decomposition, and n is the number of D4 molecules. By integrating Eq. (2), the evolution of the number of D4 molecules with time is obtained as follows:

$$n_t/n_0 = \exp[-k_{dec}(t - t_0)] \quad (3)$$

where, n_t and n_0 are the number of D4 molecules at the time of t and t_0, respectively. t_0 refers to the time when D4 begins to decompose. These results are consistent with the experimental results in fast flow reactors[7], which indicates that single-molecule decomposition is the dominant pathway for D4 pyrolysis.

Based on the first-order kinetic model, the reaction rate constant k_{dec} values at various temperatures were calculated (Fig. 8a). The results show that there is a significant linear relationship between $\ln(k_{dec})$ and 1/T ($R^2 > 0.9$), which verifies that the pyrolysis reaction follows the Arrhenius equation: $k_{dec} = A \cdot \exp(-Ea/R/T)$. In order to investigate the effects of reaction conditions, the k_{dec} of this study was analyzed jointly with the experimental data from Sanogo et al.[7] (1,058–1,197 K, ~18 mbar), and Sela et al.[12] (1,160–1,600 K, ~ 2.0 bar) (Fig. 8b). In these middle-low-temperature and low-pressure experiments, the obtained reaction rate constants are much smaller than the high-temperature and high-pressure simulated values in this work, and at some of the same temperature points (such as 1,500 K), the deviation is over 50%. This indicates that the increase in temperature and pressure can greatly promote the thermal decomposition of D4.

By fitting the reaction rate constants obtained by ReaxFF MD simulations at 1,500~2,600 K, the apparent activation energy *Ea* of D4 decomposition is found to be 81.3 ± 4.2 kJ/mol, which is significantly lower than that of Davidson et al.'s[11] low temperature static reactor experiment (301 kJ/mol), Sanogo & Zachariah's fast flow reactor experiment (about 320 kJ/mol), and Sela et al.'s shock tube experiment (273.2 kJ/mol). The difference is due to the high temperature (1,500–2,600 K) and the high pressure (~80 bar) employed in this study, which is quite different from the experimental conditions (< 1,500 K, < 2.0 bar) in the references[7,12]. This may reveal the contribution of new reaction channels at high temperature and high pressure. Figure 9 shows the main paths of D4 initial thermal decomposition by reaction trajectory analysis of ReaxFF MD simulations. It is found that there are totally five reaction paths for D4 initial decomposition, where the paths ① to ④ had been reported in the past[12]. A new reaction channel ⑤ (i.e., Si-C bond homolysis) is found in this work by ReaxFF MD simulations. Also, at the current conditions of high temperature and high pressure, the reaction paths ③ and ④ that radicals participatein are significantly enhanced due to the existence of a great amount of free radicals ($\cdot CH_3$ and $\cdot H$) in the reactive system. The total percentage of these two reaction paths reaches 70%. While the activation energies of these two reaction paths are relatively low, 76 kJ/mol, and 25.6 kJ/mol[12], respectively. Consequently, the fitted activation energy of 81.3 kJ/mol is obtained and essentially characterizes the effective apparent activation energy of the initial thermal decomposition of D4.

In addition, the effective pre-exponential factor can be obtained by intercept calculation of the fitting line, and gives $\ln A = (27.15 \pm 1.35)$ (unit of A: s^{-1}). A high A value indicates that the pyrolysis of D4

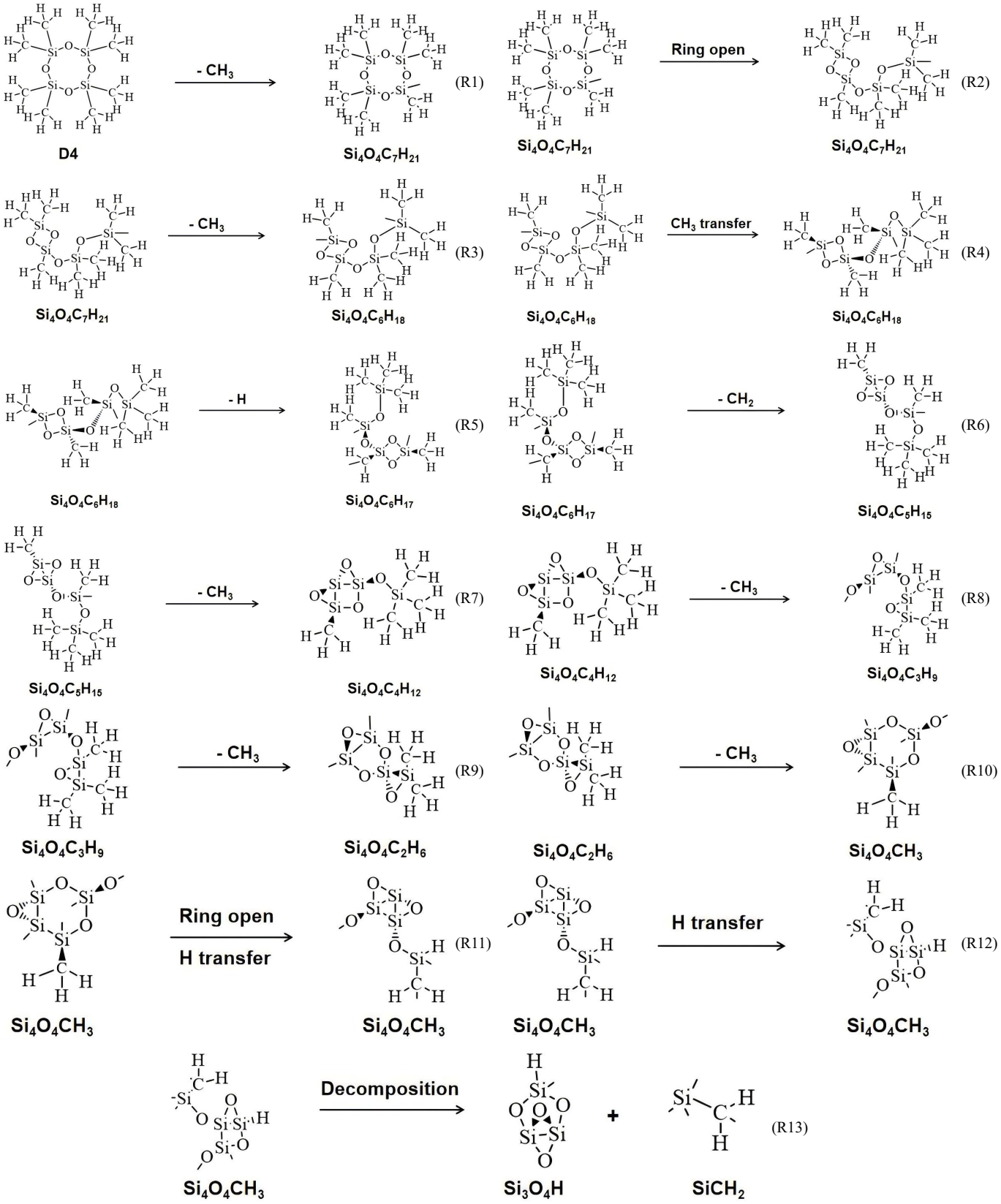

Fig. 5 Pyrolysis pathways of a single D4 molecule at 2,000 K.

involves complex transition state structure, which is consistent with the multi-step reaction characteristics of D4 thermal decomposition.

Combining the single-molecule simulation results, the microscopic mechanism of temperature effects on reaction pathways is elucidated as follows: (1) Initial bond cleavage selectivity. Above 1,500 K, Si-C bond cleavage (bond energy 377 kJ/mol) remains the primary initiation step (R1), but the rate of ring-opening reactions (Si-O cleavage) significantly increases. High temperatures enhance

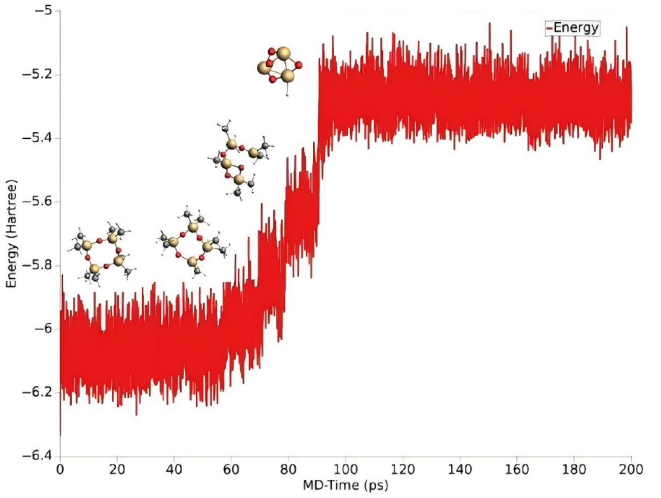

Fig. 6 Energy evolution during a single D4 molecule pyrolysis at 2,000 K.

molecular internal energy transfer, promote the release of strain energy in rigid-ring structures, and accelerate ring-opening reactions, forming linear siloxane intermediates (e.g., -$Si_4O_4C_8H_{24}$). (2) Enhanced free radical chain reactions. The concentration of methyl radicals (·CH_3) sharply rises at high temperatures (R1/R3/R6 in Fig. 5), leading to two acceleration effects: direct hydrogen extraction (·CH_3 + R-H → CH_4 + R·, where R is silicon or hydrocarbon), explaining the sudden increase in CH_4 at 843 K; and secondary cracking catalysis, where free radicals attack intermediates (e.g., open-chain siloxanes), inducing Si-O/Si-C bond homolysis and forming an autocatalytic cycle. (3) Competition for methane generation channels. At temperatures exceeding 2,000 K, Si-C bond homolysis (R1) coexists with intramolecular rearrangements (e.g., methyl migration of R4), generating H and CH_2, which contribute to methane formation via CH_2 + H_2 → CH_4, aligning with the C1/C2 product ratio changes in GC results.

Mechanism of CH_4 generation

The formation of methane (CH_4) during the pyrolysis of D4 is a critical process that exhibits strong temperature dependence, as revealed by both experimental and molecular dynamics (MD) simulation results. This section elucidates the mechanistic pathways for CH_4 generation, integrating insights from flow tube experiments (803–843 K) and ReaxFF MD simulations (1,500–2,600 K), and highlights the key reaction steps and their kinetic implications.

Based on experimental findings, it was found that CH_4 was undetectable at 803 K, while C2-C4 hydrocarbons (e.g., ethane, ethylene) dominated the product spectrum. At 843 K, CH_4 production increased dramatically, indicating a high activation energy threshold (> 803 K) for its formation. This suggests that CH_4 generation is initiated by temperature-sensitive bond cleavages (e.g., Si–C homolysis) or radical-driven pathways. In addition, from ReaxFF MD simulation results, CH_3 and CH_4 formation became significant above 1,500 K, with their yields increasing exponentially with temperature (Fig. 10).

Also, by reaction event counting of CH_4 formation across the trajectories of MD simulation at 2,000 K, 11 reactions are identified involved in CH_4 generation during the D4 pyrolysis process. Of these, ten reactions result in CH_4 production via CH_3 hydrogen abstraction, comprising about 91% of the total. The frequency of CH_4 production events is 19, with 18 instances attributed to CH_3 hydrogen abstraction, making up approximately 94.7% (details about these reactions can be found in the Supplementary File 1).

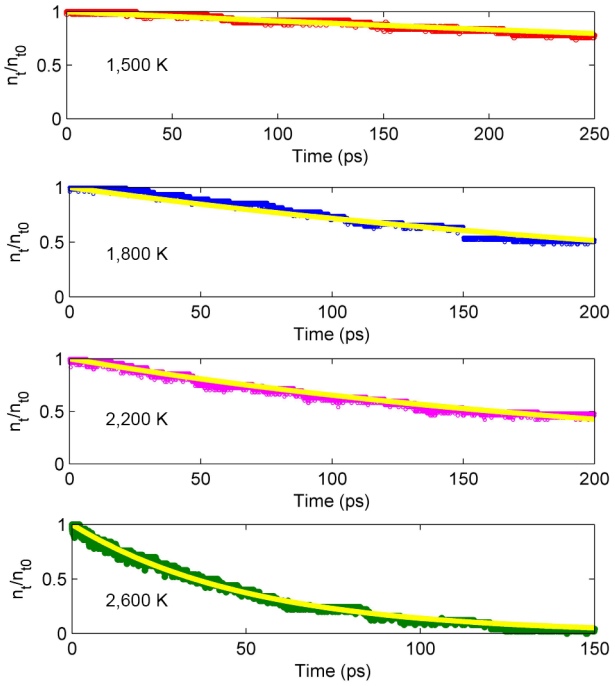

Fig. 7 Evolution of D4 molecular number at the temperature of 1,500–2,600 K. The solid line represents data fitting.

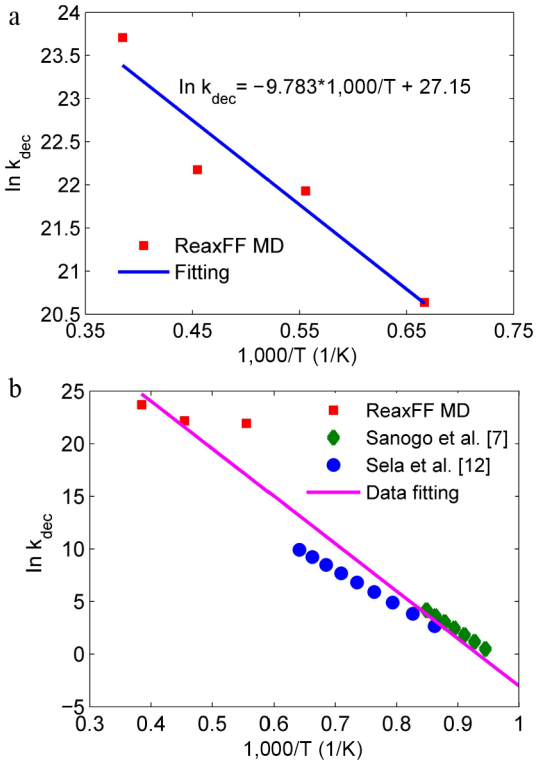

Fig. 8 Reaction rate constants of D4 pyrolysis at the temperatures of (a) 1,500–2,600 K by ReaxFF MD simulations, and (b) 1,058–2,600 K from the references.

Therefore, the simulations identified methyl radicals (·CH_3) as the primary precursor for CH_4, consistent with the experimental hypothesis of radical-mediated pathways. Based on the combined evidence, the following mechanistic routes are proposed:

(1) Si-C bond homolysis and methyl radical release represent the primary reaction pathway: Si-CH_3 → Si· + ·CH_3. The relatively weak

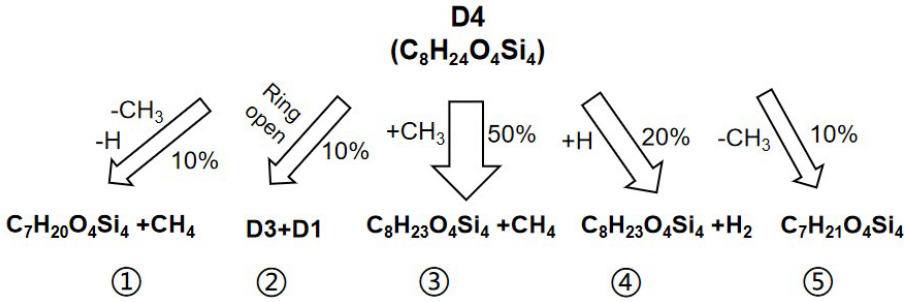

Fig. 9 Initial thermal decomposition paths of D4.

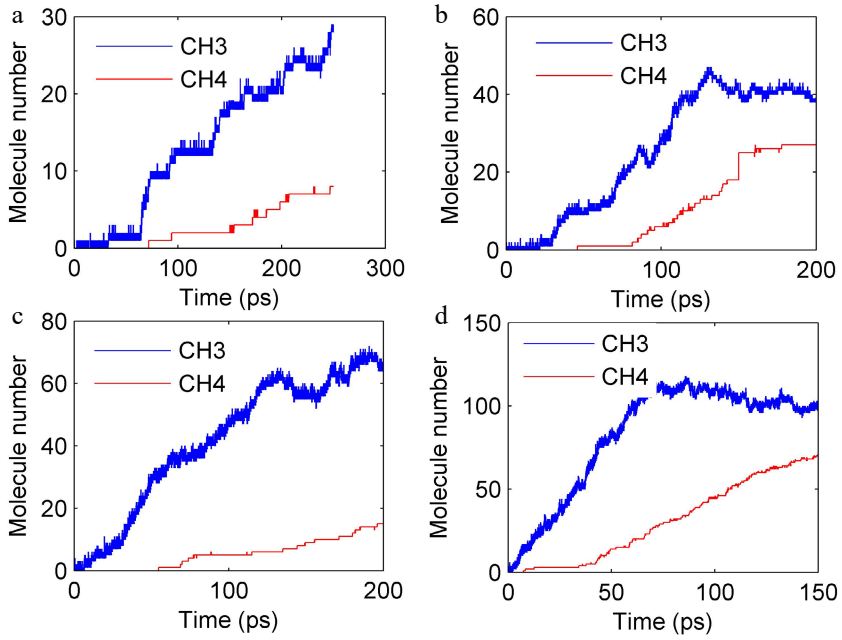

Fig. 10 Evolution of CH_4 and CH_3 molecules number at different temperatures. (a) 1,500 K, (b) 1,800 K, (c) 2,200 K, and (d) 2,600 K.

Si-C bond (377 kJ/mol) preferentially dissociates at elevated temperatures, liberating $\cdot CH_3$ radicals. This cleavage is rate-limiting at temperatures such as 803 K, but becomes relatively fast above 843 K. ReaxFF MD simulations validate that Si-C bond cleavage (R1 in Fig. 5) is the principal initiation step, with $\cdot CH_3$ concentrations showing a strong correlation with CH_4 yields (Fig. 10).

(2) Hydrogen abstraction by methyl radicals occurs as follows: $\cdot CH_3 + R\text{-}H \rightarrow CH_4 + R\cdot$ (where R is a Si- or hydrocarbon fragment). This chain-propagation step has a low activation barrier, accounting for the sharp increase in CH_4 observed at 843 K in experiments. The reaction is driven by high $\cdot CH_3$ concentrations at elevated temperatures. Both experimental and simulation data show CH_4 formation coinciding with $\cdot CH_3$ accumulation (Fig. 10). ReaxFF MD simulations also indicate that $\cdot CH_3$ abstracts hydrogen from intermediates such as open-chain siloxanes (e.g., l-$Si_4O_4C_8H_{24}$).

Intramolecular rearrangement and secondary cracking involve methyl migration and dehydrogenation, exemplified by reactions like R4 in Fig. 5, which generates CH_2 and H. These intermediates recombine to form CH_4 ($CH_2 + H_2 \rightarrow CH_4$). Secondary cracking of C2-C4 hydrocarbons (e.g., $C_2H_6 \rightarrow \cdot CH_3 + \cdot CH_3$) provides additional $\cdot CH_3$ for hydrogen abstraction. Above 2,000 K, these pathways prevail in simulations, consistent with experimental findings of extensive pyrolysis at 843 K.

At lower temperatures (803 K), CH_4 is absent due to insufficient energy for Si-C bond homolysis and limited $\cdot CH_3$ availability, with C2-C4 products forming via Si-O cleavage and methyl recombination. In contrast, at higher temperatures (≥ 843 K), Si-C cleavage accelerates, releasing $\cdot CH_3$, and radical chain reactions and intramolecular rearrangements enhance CH_4 production. The experimental detection of CH_4 at 843 K corroborates MD-predicted $\cdot CH_3$-mediated pathways. Simulations accurately reproduced the Arrhenius parameters (Ea = 81.3 kJ/mol, ln A = 27.15), confirming the predominance of radical-driven mechanisms at elevated temperatures.

In summary, CH_4 generation during D4 pyrolysis is governed by two temperature-dependent regimes: (1) Below 803 K, CH_4 formation is kinetically inhibited due to high Si-C cleavage barriers. (2) Above 843 K, Si-C homolysis and radical chain reactions prevail, with $\cdot CH_3$ hydrogen abstraction as the main CH_4 source. These findings refine kinetic models by integrating high-temperature pathways and highlight the significance of $\cdot CH_3$ dynamics in predicting CH_4 yields for industrial applications, such as silicon-based material synthesis and waste gas combustion.

Conclusions

This study elucidates the high-temperature pyrolysis kinetics of D4 through a combined experimental and ReaxFF MD simulation approach. Flow tube experiments identified a temperature-dependent transition in product distribution, with CH_4

formation becoming significant only above 843 K, underscoring the role of Si-C bond cleavage and radical-driven pathways. ReaxFF simulations revealed first-order decomposition kinetics (1,500–2,600 K) with an apparent activation energy of 81.3 kJ/mol, markedly lower than low-temperature literature values, due to the enhancement of the D4 decomposition channel that radicals participate at high temperatures. The simulations further validated $\cdot CH_3$ as the key intermediate for CH_4 production, aligning with experimental observations. These findings resolve longstanding discrepancies in D4 pyrolysis mechanisms and provide a robust kinetic framework for industrial applications at high temperatures, such as silicon nanomaterial synthesis and landfill gas combustion modeling. Future work should extend experimental validation to higher temperatures and explore the role of pressure effects on pathway selectivity.

Author contributions

The authors confirm contribution to the paper as follows: study conception and design, draft manuscript preparation: Wang N, Huang Y; data collection: Wang N, Sun J, Huang Y; analysis and interpretation of results: Wang N, Sun J, Huang Y, Shen G. All authors reviewed the results and approved the final version of the manuscript.

Data availability

The datasets generated during and analyzed during the current study are available from the corresponding author on reasonable request.

Acknowledgments

The authors express their gratitude to the support from Soochow Municipal laboratory for low carbon technologies and industries.

Conflict of interest

The authors declare that they have no conflict of interest.

Supplementary information accompanies this paper online at: https://doi.org/10.48130/prkm-0026-0008.

Dates

Received 22 July 2025; Revised 24 January 2026; Accepted 4 March 2026; Published online 8 June 2026

References

[1] Franke J, Liedke MO, Schäfer A, Butterling M, Attallah AG, et al. 2026. Comparison of the coating structure of silicon-based PECVD coatings with varying organic content. *Plasma Processes and Polymers* 23(3):e70107

[2] Huang Y, Chen H. 2024. A detailed reaction mechanism for hexamethyldisiloxane combustion via experiments and ReaxFF molecular dynamics simulations. *International Journal of Chemical Kinetics* 56(3):131–149

[3] Chen Y, Chen H, Wang J, Huang Y. 2022. Chemical kinetics of hexamethyldisiloxane pyrolysis: a ReaxFF molecular dynamics simulation study. *International Journal of Chemical Kinetics* 54(7):413–423

[4] Yeob J, Hong SW, Koh WG, Park I. 2024. Enhanced mechanical and thermal properties of polyimide films using hydrophobic fumed silica fillers. *Polymers* 16(2):297

[5] Feroughi OM, Deng L, Kluge S, Dreier T, Wiggers H, et al. 2017. Experimental and numerical study of a HMDSO-seeded premixed laminar low-pressure flame for SiO_2 nanoparticle synthesis. *Proceedings of the Combustion Institute* 36:1045–1053

[6] Chrystie RSM, Janbazi H, Dreier T, Wiggers H, Wlokas I, et al. 2019. Comparative study of flame-based SiO_2 nanoparticle synthesis from TMS and HMDSO: SiO-LIF concentration measurement and detailed simulation. *Proceedings of the Combustion Institute* 37:1221–1229

[7] Sanogo O, Zachariah MR. 2007. Fast-flow reactor study of the thermal decomposition of the octamethylcyclosiloxane (D4). *Comptes Rendus Chimie* 10:518–523

[8] Schwind RA, Wooldridge MS. 2020. Effects of organic silicon compounds on syngas auto-ignition behavior. *Combustion and Flame* 212:234–241

[9] Meng Q, Solar M, Sophonrat N, Wooldridge M. 2025. Quantitative longitudinal assessment of volatile organic silicon compounds in biogas from landfills and wastewater treatment plants. *Waste Management* 204:114950

[10] de Oliveira JCA, de Mesquita YM, Silvino PFG, Magalhaes ML, Lucena SMP. 2026. Prediction of siloxane adsorption in activated carbons by molecular simulation. *Chemical Engineering Communications* 213(4):735–743

[11] Davidson IMT, Thompson JF. 1975. Kinetics of the thermolysis of octamethylcyclotetrasiloxane in the gas phase. *Journal of the Chemical Society, Faraday Transactions 1: Physical Chemistry in Condensed Phases* 71:2260–2265

[12] Sela P, Peukert S, Herzler J, Schulz C, Fikri M. 2020. Shock-tube study of the decomposition of octamethylcyclotetrasiloxane and hexamethylcyclotrisiloxane. *Zeitschrift für Physikalische Chemie [International Journal of Research in Physical Chemistry and Chemical Physics]* 234(7-9):1395–1426

[13] Khabashesku VN, Kerzina ZA, Maltsev AK, Nefedov OM. 1989. Matrix IR spectroscopic study of the vacuum pyrolysis of octamethylcyclotetrasiloxane, allyloxy- and allyl(allyloxy)dimethylsilanes as well as 2, 2, 6-trimethyl-2-silapyrane as potential sources of dimethylsilanone. *Journal of Organometallic Chemistry* 364:301–312

[14] Almond MJ, Becerra R, Bowes SJ, Cannady JP, Ogden JS, et al. 2008. A mechanistic study of cyclic siloxane pyrolyses at low pressures. *Physical Chemistry Chemical Physics* 10:6856–6861

[15] Tian S, Yang D, Wu Y, Li C, Liu B, et al. 2025. Molecular dynamics simulation of pyrolysis in polyethylene cable sheaths under electric field. *Progress in Reaction Kinetics and Mechanism* 50:e019

[16] van Duin ACT, Dasgupta S, Lorant F, Goddard WA. 2001. ReaxFF: a reactive force field for hydrocarbons. *The Journal of Physical Chemistry A* 105:9396–9409

[17] Chenoweth K, Cheung S, van Duin ACT, Goddard WA, Kober EM. 2005. Simulations on the thermal decomposition of a poly(dimethylsiloxane) polymer using the ReaxFF reactive force field. *Journal of the American Chemical Society* 127:7192–7202

[18] Chen S, Liu C, Li Q, Liu Y, Xin L, et al. 2022. A ReaxFF-based molecular dynamics study of the pyrolysis mechanism of hexamethyldisiloxane. *Journal of Molecular Liquids* 356:119026

[19] Chen S, Liu C, Xin L, Yu W, Li Q, et al. 2023. Oxidation decomposition mechanism of hexamethyldisiloxane. *Journal of Molecular Liquids* 375:121362

Copyright: © 2026 by the author(s). Published by Maximum Academic Press, Fayetteville, GA. This article is an open access article distributed under Creative Commons Attribution License (CC BY 4.0), visit https://creativecommons.org/licenses/by/4.0/.